Materials Transactions, Vol. 57, No. 6 (2016) pp. 860 to 864
Special Issue on Frontier Researches Related to Interconnection, Packaging and Microjoining Materials and Microprocessing for Such Materials

Reliable Material Properties of Aluminum Pads with Strong Delamination Toughness in Gold - Aluminum Wire Bonding

Toru Ikeda* and Kenta Shiba

Department of Mechanical Engineering, Kagoshima University, Kagoshima 890–0065, Japan

Au/Al wire bonding is the traditional bonding method of circuits of electronic packages, and still a very important bonding technique. Bonding strength was measured by the shear test of a gold ball on an aluminum pad. Delamination behavior was categorized into three types, cohesive fracture in the gold ball, interfacial delamination between the gold ball and the aluminum pad, and fracture from inside of the aluminum pad. The cohesive fracture in the gold ball is the most reliable in these three types of fracture. We investigated the mechanisms causing the different types of fracture from the shear test. First, we observed the surface of aluminum pads using a scanning electron microscope (SEM) and measured the orientation of crystal grains using the electron backscatter diffraction (EBSD). A porous structure was observed on the surface of the aluminum pad that caused the fracture from the inside of the pad. Almost all of the crystal grains on the aluminum pads were aligned (111). Then, we measured the material properties of aluminum pads using a nano-indenter. Aluminum pads with stiff surfaces showed interfacial fracture. Aluminum pads with soft surfaces and large absorbed plastic energy showed cohesive fracture of the gold balls.
[doi:10.2320/matertrans.MD201502]

(Received November 30, 2015; Accepted February 12, 2016; Published April 1, 2016)

Keywords: *Wite Bonding, Aluminum Pad, EBSD, Nano-Indentation*

1. Introduction

Interconnecting techniques are very important for electronic products. Wire bonding is one of the traditional techniques for the interconnection in electronic devices, and it is still often used. Gold wire and copper wire are often used for the wire bonding. Au/Al wire bonding is the most typical combination of the wire bonding.

Au/Al wire bonding process can be divided into two processes, the first bonding between the gold wire and the aluminum terminal on a silicon chip and the second bonding between the gold wire and the outer terminal. In this study, we focused on the first bonding process of Au/Al wire bonding.

In the first bonding process, the gold ball is formed at the top of a capillary tool. Then the gold ball is impressed on the aluminum terminal and vibrated by ultra sonic at the top of a capillary. Due to the vibration, the oxide layer on the aluminum terminal is broken and the intermetallic compound (IMC) is formed between the gold ball and the aluminum terminal[1]. The IMC causes the strong bonding between the gold ball and the aluminum terminal.

The Au/Al wire bonding is sometimes broken during the operation or the assembling. The strength of the Au/Al wire bonding strongly depends on the properties of aluminum terminals. We investigated the material properties of aluminum pads which cause the strong Au/Al wire bonding.

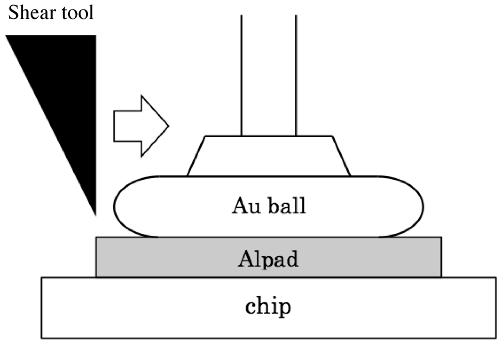

Fig. 1 Shear test of Au/Al wire bonding.

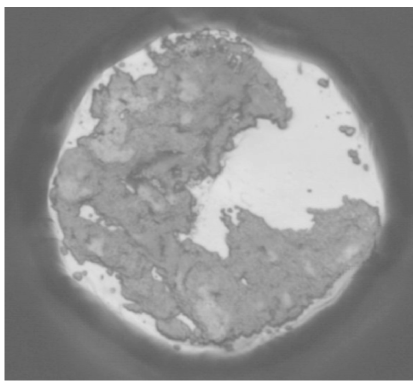

Fig. 2 IMC remaining on the surface of a bonded gold ball.

2. Shear Tests

We performed the shear test as shown in Fig. 1 for five samples of Au/Al wire bonding. The diameter of Au wire was 30 μm, the impressing load was 30 gf, the ultrasonic frequency and amplitude were 120 kHz and 0.4 μm respectively, and the temperature of specimens was 230°C for all samples. We judged the cohesive fracture in the gold ball to be good bonding. The interfacial fracture and the fracture from the inside of an aluminum terminal are not good bonding. The IMC alloying rate was measured as the rate of IMC area covered on the surface of a gold ball as shown in Fig. 2. In Fig. 2, an aluminum pad was dissolved using acid. Fracture pattern and IMC alloying rate for five samples are shown in Table 1.

In this Table, Sample 1 and Sample 5 showed desirable bonding strength, because the cohesive fracture happened in

*Corresponding author, E-mail: ikeda@mech.kagoshima-u.ac.jp

Table 1 Fracture patterns of shear tests and IMC remaining rate on surfaces of gold balls.

	Sample 1	Sample 2	Sample 3	Sample 4	Sample 5
Pad structure	Al:1.5µm substrate	AlSiCu:1.5µm Barrier metal substrate	AlCu:1.5µm Barrier metal AlCu:3µm substrate	AlCu:1µm substrate	AlCu:1.5µm Barrier metal AlCu:1µm Barrier metal AlCu:0.5µm substrate
Total thickness of Al layer	1.5 μm	1.5 μm	4.5 μm	1 μm	3 μm
Fracture pattern of shear test	Cohesive fracture in an Au ball (Good)	Intermediate between cohesive and interface fractures	Inside of Al pad	Interface between Au and Al	Cohesive fracture in an Au ball (Good)
IMC alloying rate	Good	Marginal	Good	Marginal	Good

a gold ball and IMC remaining rate are reasonably high. To make clear the reason of the difference of these bonding strength, we investigated properties of aluminum pads using the electron back-scatter diffraction (EBSD) with a scanning electron microscope (SEM)[2] and nano-indentation tests.

3. Crystal Orientation and Size of Crystal Grains on the Surface of Aluminum Pads

We observed the surfaces of on aluminum pads using the SEM (Hitachi SU-70) and investigated the orientations of crystal grains using EBSD analysis software (TSL OIM analysis 4). We did not perform any treatments on the aluminum pads. Accelerating voltage was 15 kV and the number of EBSD sampling points were from 60000 to 80000 for respective samples. SEM observation photographs and EBSD analysis results are shown in Figs. 3 (a)–3 (e).

Orientations of surface crystal grains were aligned almost (111) direction. The gaps of crystal grains in Sample 1 are relatively narrow and the crystal grains have no voids. Sample 2 has many voids in respective crystal grains. Sample 3 has wide gaps between crystal grains and has porous structures in the crystal grains. In Sample 4, crystal grains are smaller than other sample's. In Sample 5, gaps between crystal grains are relatively wide, but each crystal grain has no void.

4. Nano-Indentation Test

To investigate the material properties of respective samples of aluminum pads, we performed Nano-indentation tests. We used a Nano-indenter (ELIONIX ENT-2100).

Schematic of indentation h (depth) – P (load) curve is shown in Fig. 4. The h-P curve generally follows Kick's law as

$$P = Ch^2, \tag{1}$$

where C is the loading curvature. The maximum indentation depth h_m occurs at P_m.

Initial unloading slope is defined as $\left|\frac{dP_u}{dh}\right|_{h_m}$, where P_u is unloading force. W_e and W_p are the elastic work during unloading and plastic work during loading respectively. $W_t = W_p + W_e$ is total work. The residual indentation depth after unloading is h_r.

Indentation depth (h) - Load (P) curves for respective samples are shown in Figs. 5 (a)–5 (e). We obtained W_p/W_t, $\left|\frac{dP_u}{dh}\right|_{h_m}$ and C from h-P curves in Figs. 5 (a)–5 (e) as shown in Table 2. The elastic-plastic stress-strain curve of a material is assumed to be

$$\sigma = \begin{cases} E\varepsilon, & \text{for } \sigma \leq \sigma_{ys} \\ R\varepsilon^n, & \text{for } \sigma \geq \sigma_{ys} \end{cases} \tag{2}$$

where E is Young's modulus, R a strength coefficient, n the strain hardening exponent, σ_{ys} is the yield stress.

Young's modulus (E), yield stress (σ_{ys}) and strain hardening exponent (n) of each aluminum pad are obtained from W_p/W_t, $\left|\frac{dP_u}{dh}\right|_{h_m}$ and C using the reverse analysis proposed by Dao et al.[3] as shown in Table 2.

The hardness, H_{IT},[4,5] of material is defined as the ratio between normal force P_m and projected contact area A_p as

$$H_{IT} = \frac{P_m}{A_p}. \tag{3}$$

The projected contact area A_p for Berkobich indenter is shown as

$$A_p = 24.56 \times h_c^2, \tag{4}$$

where h_c is the depth of the contact of the indenter with the test piece at P_m. h_c is

$$h_c = h_m - \gamma \frac{P_m}{\left|\frac{dP_u}{dh}\right|_{h_m}}, \tag{5}$$

where γ is a parameter depending on the indenter, $\gamma = 0.75$ for Berkobich indenter. The hardness H_{IT} has the relationship with Vickers hardness as

$$HV = 0.0924 \times H_{IT}. \tag{6}$$

H_{IT} and HV for respective samples are shown in Table 3.

In Figs. 5 (a)–5 (e), the indentation load increased discontinuously in many cases. The reason of discontinuity is not clear. It has been discussed in terms of the oxide film, an unknown contamination layer on the sample surface and the nu-

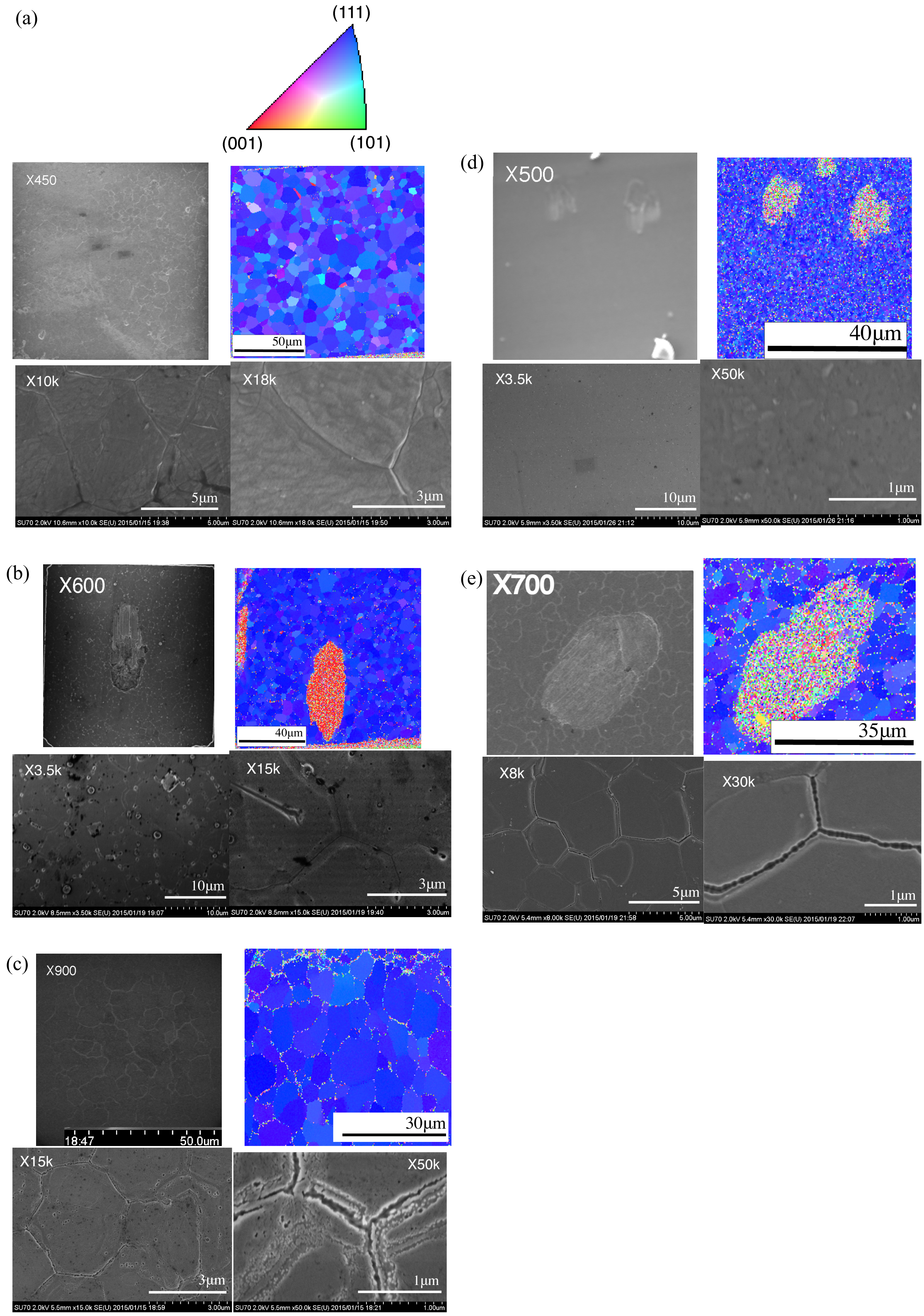

Fig. 3 (a) SEM and EBSD images for Sample 1, (b) SEM and EBSD images for Sample 2, (c) SEM and EBSD images for Sample 3, (d) SEM and EBSD images for Sample 4, (e) SEM and EBSD images for Sample 5.

cleation and emission of dislocations[6]. Table 2 shows material properties of respective aluminum pads obtained from the nano-indentation data using reverse analysis proposed by Dao et al.[3]. In these material properties, Young's modulus is relatively reliable, but yield stress σ_{ys} and strain hardening component n are not reliable[3]. Young's modulus of bulk aluminum is about 70 GPa. All samples have lower Young's moduli than that of balk aluminum.

IMC remaining rates of Samples 1, 3, 5 in Table 1 are good. Young's moduli of these samples are less than 20 GPa (Table 2) and hadnesses H_{IT} are less than 1500 MPa (Table 3). Soft aluminum structures can be easily slid by ultrasonic vibration and the oxide layers are broken. Appeared fresh aluminum surfaces make thick layers of intermetallic compound with gold. A thick IMC layer makes good bonding. However, Sample 3 caused the failure of aluminum pad. Young's modulus and W_p/W_t of Sample 3 are especially small. According to Fig. 3 (c), it looks porous structure. This pad is too brittle and week.

IMC remaining rate of Sample 4 in Table 1 is marginal. Young's modulus of this sample is high and close to balk aluminum. H_{IT} of this sample is also very high. Hard aluminum structure cannot be slid by ultrasonic vibration and the oxide layer is not fully broken. The IMC layer does not grow up well. Under the shear test, this sample was broken along the interface between an aluminum pad and a gold ball.

IMC remaining rate of Sample 2 in Table 1 is also margin-

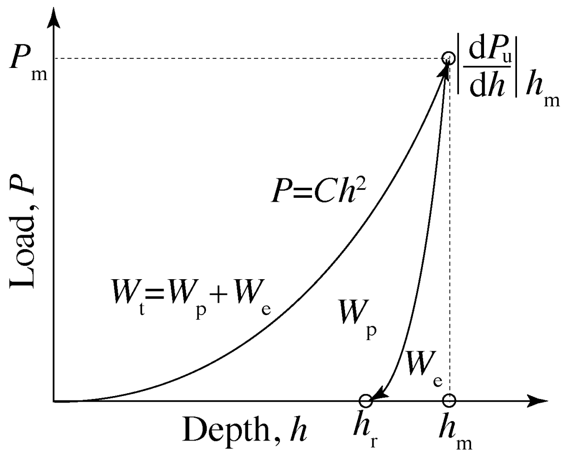

Fig. 4 Schematic of h (indentation depth) – P (load) curve.

Table 2 Material properties of aluminum pads obtained by a nano-indenter.

	W_p/W_t	$\left.\left\lvert\frac{dP_u}{dh}\right\rvert\right\rvert_{h_m}$	C	E (GPa)	σ_{ys} (MPa)	n
Sample 1	0.923	13.47	6.48	17.0	93.7	0.178
Sample 2	0.866	15.31	15.16	27.4	211.5	0.130
Sample 3	0.361	1.79	8.35	4.8	339.5	-
Sample 4	0.822	17.88	68.82	60.0	1632	0
Sample 5	0.916	17.00	19.35	19.3	491.7	0

E: Young's modulus; σ_{ys}: Yield stress; n: Strain hardening exponent

Table 3 Hardness of aluminum pads.

	Sample 1	Sample 2	Sample 3	Sample 4	Sample 5
H_{IT} (MPa)	1487	1800	937	4675	1355
HV	137.4	166.3	86.6	432.0	125.2

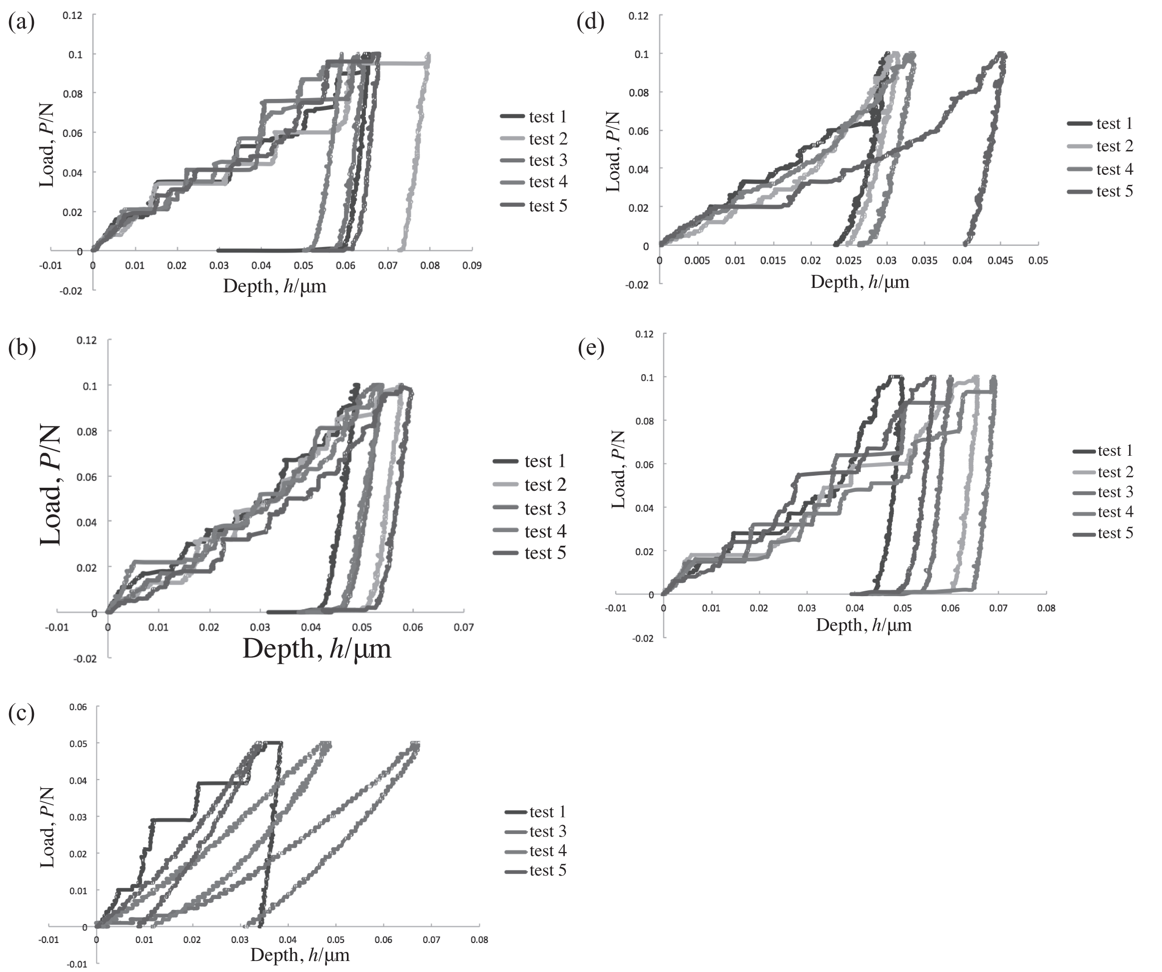

Fig. 5 (a) h-P curves for Sample 1, (b) h-P curves for Sample 2, (c) h-P curves for Sample 3, (d) h-P curves for Sample 4, (e) h-P curves for Sample 5.

al. Young's modulus and H_{IT} of this sample are intermediate between Samples 1, 3, 5 and Sample 4. A part of broken surface is cohesive fracture in a gold ball, but remaining part are interfacial failure between aluminum pad and a gold ball.

5. Conclusion

We performed the shear test of Au wire bonded aluminum pads to investigate shear strength. Aluminum pads were dissolved from the Au wire bonded aluminum pads to measure the remaining rate of IMC layers on the gold ball.

To investigate the reasons of results, material properties of five kinds of aluminum pads were measured using a SEM with EBSD and nano-indentation test. We obtained following information of material properties influencing the quality of Au-Al wire bonding.

(1) Orientation of crystal grains on the surfaces of aluminum pads are aligned almost (111) for all samples.
(2) Soft aluminum pads whose Young's moduli are less than 20 GPa and hardness H_{IT} are less than 1500 MPa make thick IMC layers.
(3) Too soft aluminum pad whose structure is pours is brittle. It causes the failure from the inside of an aluminum pad during the shear test.
(4) Too hard aluminum pad whose Young's modulus is larger than 50 GPa and Hardness H_{IT} is larger than 4000 MPa cannot make a thick IMC layer. It results in the interfacial failure between an aluminum pad and a gold ball.

REFERENCES

1) J. DeLucca, J. Osenbach and F. Baiocchi: J. Electron. Mater. **41** (2012) 748–756.
2) T. Maitland and S. Sizman, Electron Backscatter Diffraction (EBSD) Technique and Materials Characterization Example, Scanning Microscopy for Nanotechnology (2007), pp. 41–75.
3) M. Dao, N. Chollacoop, K.J. Van Vliet, T.A. Venkatesh and S. Suresh: Acta Mater. **49** (2001) 3899–3918.
4) Metallic materials – Instrumented indentation test for hardness and material parameters – Part I: Test method, ISO 14577-1 (2002).
5) J.L. Bucaille, S. Stauss, E. Felder and J. Michler: Acta Mater. **51** (2003) 1663–1678.
6) M. Yoshida, T. Sumomogi, T. Endo, H. Maeta and T. Kino: Mater. Trans. **48** (2007) 1–5.